

ACCEPTED MANUSCRIPT

Giant thermopower in 'p' type OsX_2 (X: S, Se, Te) for a wide temperature range: A first principles study

To cite this article before publication: Sreeparvathy P C *et al* 2018 *J. Phys.: Condens. Matter* in press <https://doi.org/10.1088/1361-648X/aaca6a>

Manuscript version: Accepted Manuscript

Accepted Manuscript is "the version of the article accepted for publication including all changes made as a result of the peer review process, and which may also include the addition to the article by IOP Publishing of a header, an article ID, a cover sheet and/or an 'Accepted Manuscript' watermark, but excluding any other editing, typesetting or other changes made by IOP Publishing and/or its licensors"

This Accepted Manuscript is © 2018 IOP Publishing Ltd.

During the embargo period (the 12 month period from the publication of the Version of Record of this article), the Accepted Manuscript is fully protected by copyright and cannot be reused or reposted elsewhere.

As the Version of Record of this article is going to be / has been published on a subscription basis, this Accepted Manuscript is available for reuse under a CC BY-NC-ND 3.0 licence after the 12 month embargo period.

After the embargo period, everyone is permitted to use copy and redistribute this article for non-commercial purposes only, provided that they adhere to all the terms of the licence <https://creativecommons.org/licenses/by-nc-nd/3.0>

Although reasonable endeavours have been taken to obtain all necessary permissions from third parties to include their copyrighted content within this article, their full citation and copyright line may not be present in this Accepted Manuscript version. Before using any content from this article, please refer to the Version of Record on IOPscience once published for full citation and copyright details, as permissions will likely be required. All third party content is fully copyright protected, unless specifically stated otherwise in the figure caption in the Version of Record.

View the [article online](#) for updates and enhancements.

Giant thermopower in 'p' type OsX_2 (X: S, Se, Te) for a wide temperature range: A first principles study

P. C. Sreeparvathy and V. Kanchana*

¹Department of Physics, Indian Institute of Technology Hyderabad, Kandi - 502 285, Sangareddy, Telangana, India.

E-mail: kanchana@iith.ac.in

Abstract. We report the electronic structure and thermoelectric (TE) properties of OsX_2 (X: S, Se, Te), and find a giant value of thermopower of magnitude $600 \mu\text{VK}^{-1}$ to $800 \mu\text{VK}^{-1}$ for a wide temperature range of 100 K - 500 K for hole doping (at 10^{18}cm^{-3}), which is higher than the value found for well established TE materials. The optimized structural parameters are in good agreement with available experimental reports. The mechanical stability of all the compounds are confirmed from the computed elastic constants. The band gap of the investigated compounds is examined by several exchange correlation functionals, and TB-mBJ with modified parameters is found to be the best. The heavy valence bands stimulates the thermopower value for hole doping and light conduction bands intensifies the electrical conductivity values for electron doping, enabling both 'n' and 'p' type doping favourable for TE applications at higher concentrations (10^{20}cm^{-3}), which brings out the device application. Our results unveil the possibility of TE applications for all the examined compounds for a wide temperature range (100 K to 500 K), and OsS_2 specifically is quite alternative with the performing temperature ranging from 100 K - 900 K.

Keywords: Electronic structure, thermoelectric properties

1. Introduction

Transition metal chalcogenides and pnictides possess diverse structural, electronic properties, and stand in the forefront of various applications[1, 2, 3, 4]. These compounds in general possess van der Waals layered structure (MoS₂ type) or 3D like structure (pyrite/marcasite). The structural and chemical properties of these two series are well investigated. The 2D like materials are quite attractive because of their nano-level applications[5, 6], and significant number of compounds from pyrite/marcasite family have been investigated for their electronic, optical, thermoelectric and photovoltaic applications[7, 8]. Moreover, pyrite to marcasite structural transitions are also observed under pressure in several materials like FeS₂[9]. However Os based dichalcogenides and pnictides are less investigated in comparison with other TMDs. Crystal structure and Raman spectra of Os based dichalcogenides has been examined in the very early stage, where they confirmed the pyrite structure, whereas, Os based pnictides are found to crystallize in marcasite structure[10]. The band gap of both Os chalcogenides and pnictides matches the semiconducting range, and this indicate the possibility of photovoltaic and thermoelectric applications in these compounds. Conventional TMD materials, in general, host a mixture of flat and dispersed band structure[11], which further help for thermoelectric energy conversion. Yet another point to mention is that, OsS₂ (Erlichmanite) is a well known naturally occurring compound, and fall into Platinum group minerals. Other pyrite type dichalcogenides like FeS₂ are already realized as a good thermoelectric material[12], but Os based compounds are less investigated in this family. Since OsX₂ (X: S, Se, Te) are iso-structural with pyrite FeS₂, we believe that OsX₂ (X: S, Se, Te) can be explored for the investigation of electronic and thermoelectric properties.

The energy conversion using thermoelectric phenomena has attracted the scientific world consistently due to specific advantages such as absence of moving parts, less maintenance, waste heat recovery etc. Prospective materials are needed to achieve an efficient ZT (figure of merit), which is considered as the scaling parameter for every temperature. The figure of merit is defined as $ZT = S^2\sigma T/\kappa$, where S , σ , κ , and T are the thermopower, the electrical conductivity, the thermal conductivity, and the absolute temperature, respectively. κ includes both the electronic, κ_e , and the lattice contributions, κ_l , i.e., $\kappa = \kappa_e + \kappa_l$. The conflicting dependencies of thermopower and electrical conductivity over effective mass and carrier concentration makes it a great challenge in achieving good figure of merit value. Eventually researchers have to look for divergent methods to meet the demands, either by improving power-factor or by reduction of lattice thermal conductivity. The power-factor value is dependent on electronic structure derived properties such as thermopower and electrical conductivity, and we would like to examine the electronic structure and thermoelectric properties of Os based dichalcogenides OsX₂ (X:S, Se, Te) in the present work. The organization of the present manuscript is such a way that section 2 contains the details of computational methods, section 3 presents the results and discussions followed by conclusions.

2. Methods

For structural optimization, we have used pseudo potential method as implemented in Plane Wave self consistent field (Pwscf) program[13], with a plane wave cut-off 140 Ry and convergent criteria of 10^{-5} (a.u) has been used for energy minimization. The optimized lattice parameters are used for further calculations. We have used full potential linearised augmented plane wave (FP-LAPW) method as implemented in WIEN2K package [14, 15] to understand the electronic structure properties. It is well known that the traditional exchange functionals like local density approximation (LDA) and generalized gradient approximation (GGA) underestimate the band gap of semiconductors and insulators, and we have used Tran-Blaha modified Becke-Johnson (TB-mBJ) functional[16, 17] with modified parameters[18] for band gap enhancement. Due to the presence of heavy elements in the investigated compounds, we have included spinorbit coupling in our calculations. For total energy calculations, band structures and density of states, we have used 1000 k-points in the full Brillouin zone. Transport coefficients such as thermopower (S in $\mu V K^{-1}$) and electrical conductivity scaled by relaxation time (σ/τ in $\Omega^{-1} m^{-1} s^{-1}$) (will be addressed as electrical conductivity) were calculated using BoltzTraP code[19] with a dense k- mesh of $50 \times 50 \times 50$ k-points. The BoltzTraP code is based on two major assumptions such as rigid band approximation (RBA) [20, 21, 22] and the constant scattering time approximation (CSTA), and significant number of thermoelectric materials are predicted within these approximations successfully[23, 24, 25, 26, 27].

3. Results and discussions

3.1. Structural and electronic properties

The investigated compounds crystallize in pyrite structure with space group $P_a\bar{3}$ (No. 205), see Fig. 1. Bond lengths and angles are analysed for all the compounds, and are given in Table 1. The bond length between 'Os' and Os-X (X:S, Se, Te) are found to increase from OsS₂ to OsTe₂, and both bond lengths and bond angles are found to be higher than the prototype compound FeS₂[28]. The observed incremental nature in the bond length from OsS₂ to OsTe₂ might eventually reduce the interaction between atoms and lead to lesser value of Debye temperature, and further provide the possibility of reduced thermal conductivity value. The optimized lattice parameters along with available experimental reports are represented in Table 2, and from the table it is clear that optimized values are in good agreement with experimental values, and for further calculations we have used the optimized lattice parameters. Coming to electronic structure analysis, the computed band gap using different functionals are provided in Table 3, and band structure along different high symmetry directions using TB-mBJ with modified parameter are presented in Figure 2. All the investigated compounds are found to be direct band gap semiconductors with almost similar band profile, and comparable with other prototype compounds. A close analysis of the band structure of

OsS₂ reveals, the existence of flat and dispersed bands near Fermi level, and more flat bands are observed near valence band maximum compared to the vicinity of conduction band minimum, which might indicate higher value of thermopower for hole doping, and higher value of electrical conductivity for electron doping. Furthermore, the number of bands near the valence band maximum is higher than that near the conduction band minimum, and this introduces more number of bands within small energy range and will contribute for thermopower, which again gives a hint of favourable thermopower for hole doping.

It is worthy to compare the band profile of these pyrite structure with other TMDs. In the case of MoS₂, FeS₂ and Os based pnictides, both valence and conduction bands are found to be similar[11], and expected to have complementing transport properties. But in the compounds of present study, the band profile of valence and conduction bands are entirely different, and one might expect dissimilar transport properties. This significant difference in the band profile might lead to interesting TE properties of these investigated compounds, and will be discussed in the later section. From the band structure, it is clear that in valence band along Γ -X, the bands are almost flat, and along R-M the band is dispersive, whereas in the conduction band the band is dispersive along Γ -X, and less dispersive along R-M. The dispersive nature is found to increase from S to Te. This indicates the presence of heavy and light mass carriers in the band structure, which is helpful for thermoelectric properties, where heavy band mass will contribute for thermopower and light band mass will contribute for electrical conductivity. To understand the dominant states near the Fermi level, we have investigated the total and partial density of states. In Fig. 3 we have represented the density of states of all the investigated compounds. In the case of OsS₂, valence band states near Fermi level, are dominated by Os, and in conduction band, we can see a hybridisation of Os and S states. While moving from S to Te, we can see the contribution of anion increasing in valence band near Fermi level. Compared to conduction band, we can see a steep increment in density of states in valence band near Fermi level, and this indicates the dominating thermopower nature for hole doping. The extended hybridisation in the conduction band near Fermi level reveals the possibility of enhanced electrical conductivity for electron doped case compared to hole doped case. To confirm the presence of light and heavy band mass in the band structure, we have examined the effective mass in the unit of electron mass along Γ -X for both valence and conduction band, and are given in Table 4. From the table it is evident that there exist, one order of magnitude of difference in the values between valence and conduction band, which is in line with our previous discussions. In the case of other marcasite compounds the magnitude of effective mass is almost same for both valence and conduction bands.

3.2. Mechanical properties

To check the mechanical stability of these compounds, we have calculated the elastic constants, and the same is represented in Table.5. All the elastic constants for all

the compounds are found to be positive and found to satisfy Born elastic stability criteria[29], and this confirms the mechanical stability of these compounds. The C_{11} value of all the compounds are found to be higher than both C_{12} and C_{44} , which indicate the strong resistance for axial compression compared to shear compressions[30]. In addition, bulk modulus, longitudinal velocity, transverse velocity and Debye temperature are given in Table. 5. The values of elastic constants are found to higher in OsSe₂ compared to the other two compounds. The bulk modulus of all the investigated compounds are found to be comparable with prototype compounds such as FeS₂ and 'Os' based pnictides. Further, the value of Debye temperature of our investigated compounds are found to be lesser than the prototype compound FeS₂[31], indicating the thermal conductivity to be lower in these compounds[32].

3.3. Thermoelectric properties

In this section, we have examined the thermoelectric properties such as thermopower, electrical conductivity and power factor as a function of carrier concentrations and temperatures. Figure 4(a-f) represents the thermopower as a function of carrier concentrations for both holes and electrons for all the investigated compounds at different temperatures ranging from 100 K to 600 K. As anticipated from the band structure, the hole carriers are found to secure higher magnitude of thermopower for all the investigated compounds. A thermopower around $600 \mu V K^{-1}$ has been observed at 100 K for hole concentration around 10^{18}cm^{-3} for all the investigated compounds, which is huge compared to well established TE materials. In the case of OsS₂, the variation of thermopower as a function of both holes and electrons are found to be decreased with increasing carrier concentration. A maximum value of $820 \mu V K^{-1}$ is found around 600 K for hole doping. In the case of electrons, the magnitude of thermopower is found around $200 \mu V K^{-1}$ to $400 \mu V K^{-1}$ for the temperature range 100 K to 600 K, which is also appreciable. Coming to OsSe₂, the trend of thermopower is found to be similar except for the presence of bipolar conduction around 500 K[33, 34]. OsTe₂ also showed similar behaviour as other compounds. Moving to the electrical conductivity values, Figures 5(a-f) represent the electrical conductivity for hole and electron doping for all the investigated compounds. The extremely dispersed bands in the conduction bands provided a favourable conductivity for electron doping over hole doping with almost one order difference. This trend is found to be similar for all the compounds. The magnitude of electrical conductivity is found to be increased with carrier concentration. The difference in band profile of valence and conduction bands are reflected in both thermopower and electrical conductivity value for both holes and electron doping. As our attention is towards the net thermoelectric efficiency, we need to look at the parameter called power factor, and the same is given in Figure 6(a-f). The enhanced electrical conductivity for electron doping leads to an approving value of power factor for electron doping over hole doping for all the investigated compounds at lower concentrations. The vital point is that at higher concentrations around 10^{20}cm^{-3} and temperature around

600 K, both hole and electron doping secured almost similar value of power-factor, which might lead to device applications.

As discussed in the introduction, it is demanding to explore the TE materials for wide temperature range. In general, the carrier concentrations ranging from $1 \times 10^{18} \text{cm}^{-3}$ to $1 \times 10^{21} \text{cm}^{-3}$ are considerable, and now let us have a close analysis of transport properties for the same. In the first part of this section, we have pointed out the presence of bipolar conduction above 600 K for OsS_2 , and for the other two compounds its starts at little lower temperatures itself. Now let us take the case of OsS_2 , where the thermopower has reduced due to bipolar conduction only at low carrier concentrations around $\times 10^{18} \text{cm}^{-3}$, and for higher concentrations the thermopower values are appreciable. We have examined the thermopower and electrical conductivity of OsS_2 at around $2.3 \times 10^{19} \text{cm}^{-3}$ for a wide temperature range from 100 K - 900 K, and provided the same in Figure 7. For the whole temperature range, holes secured higher value of thermopower and electrons were found to possess higher value of conductivity. From the figure it is quite evident that, OsS_2 might turn to be a potential TE material for a wide temperature range. Figure 8, represent the comparison plot with other TE materials, and from the figure it is evident that the investigated compounds possess higher value of thermopower at 100 K and comparable value at room temperature and above.

Huge value of thermopower around 100 K is found with a reasonable electrical conductivity for hole doping in all the investigated compounds. The power-factor value of hole doping is found to increase as a function of carrier concentration and reach a magnitude of around 10^{11} at higher concentrations around 10^{20}cm^{-3} , which is comparable with established TE materials. If one can enhance the electrical conductivity, by preserving thermopower, through chemical doping all the investigated compounds might be promising TE material.

4. Conclusions

Electronic and thermoelectric properties of OsX_2 are analysed. Huge value of thermopwer is observed at low temperature around 100 K for hole doping for all the investigated compounds, which is found be higher than well established TE materials. The mixture of heavy and light band mass in the band structure is reflected from the band structure. Analysis of thermoelectric properties revealed the potential TE application for a wide temperature range. All the investigated compounds are favourable for electron doping at low concentrations, and for higher concentrations both carriers are preferable, which shows possible device applications for all the compounds.

5. Acknowledgement

The authors SPC and VK would like to thank IIT Hyderabad for computational facility, and SPC would like to thank MHRD for fellowship.

- [1] Wen-Hui Xie, Ya-Qiong Xu, Bang-Gui Liu and D. G. Pettifor, 2003, *Phys. Rev. Lett*, **91**, 037204.
- [2] Thomas Heine, 2015, *Acc. Chem. Res*, **48**, 65
- [3] Wen-Hui Xie, Bang-Gui Liu and D. G. Pettifor, 2003, *Phys. Rev. B*, **68**, 134407
- [4] Deep Jariwala, Vinod K. Sangwan, Lincoln J. Lauhon, Tobin J. Marks, and Mark C. Hersam, 2014, *ACS Nano*, **8** (2), 1102.
- [5] Yifei Yu, Guoqing Li, Lujun Huang, Andrew Barrette, Yong-Qing Cai, Yiling Yu, Kenan Gundogdu, Yong-Wei Zhang, and Linyou Cao, 2017 *ACS Nano*, **11**, 9390.
- [6] Hang Chen, Tianjiao Liu, Zhiqiang Su, Li Shang and Gang Wei, 2018, *Nanoscale Horiz*, **3**, 74.
- [7] Dong Gwon Moon, et.al, 2018 *Solar Energy*, **159**, 930.
- [8] Xiangli et.al, 2017 *Physica B: Condensed Matter*, **15**, 119.
- [9] Vijay Kumar Gudelli, et. al, 2013, *J. Phys. Chem. C*, **117**, 21120.
- [10] Daniel E. Bugaris, et. al, 2014 *Inorg. Chem.*, **53**, 9959.
- [11] Sohail Ahmad 1 , Sugata Mukherjee, 2014, *Graphene*, **3**, 52.
- [12] Vijay Kumar Gudelli, V. Kanchana, G. Vaitheeswaran, M. C. Valsakumar and S. D. Mahantid, 2014, *RSC Adv.*, **4**, 9424.
- [13] S. Baroni, S. D. Gironcoli and A. dal Corso et al, 2008. [http : //www.pwscf.org](http://www.pwscf.org)
- [14] P. Blaha, K. Schwarz, G. K. H. Madsen, D. Kvasnicka and J. Luitz. *WIEN2k*, An augmented plane wave +local orbitals program for calculating crystal properties, Karlheinz Schwarz, Techn. Universitat Wien, Austria (2001).
- [15] P. Blaha, K. Schwarz, P. I. Sorantin and S. B. Tricky, 1990, *Comput. Phys. Commun.*, **59**, 399.
- [16] A. D. Becke and E. R. Johnson, 2006, *J. Chem. Phys.* **124**, 221101 .
- [17] F. Tran, P. Blaha, 2009 *Phys. Rev. Lett.*, **102**, 226401 .
- [18] Radi A. Jishi, Oliver B. Ta, and Adel A. Sharif, 2014, *Phys. Chem. C*, **118**, 28344.
- [19] G. K. H. Madsen and D.J Singh, 2005, *Comput. Phys. Commun*, **67**, 175 .
- [20] T. J. Scheidemantel, C. Ambrosch-Draxl, T. Thonhauser, J. V. Badding and J.O. Sofo, 2003, *Phys. Rev. B*, **68**, 125210
- [21] L. Jodin, J. Tobola, P. P echeur, H. Scherrer and S. Kaprzyk, 2004 *Phys. Rev. B*, **70**, 184207 .
- [22] L. Chaput, P. Pecheur, J. Tobola and H. Scherrer, 2005, *Phys. Rev. B*, **72**, 085126.
- [23] K. P. Ong, D. J. Singh and P. Wu, 2011 *Phys. Rev. B*, **83**, 115110.
- [24] D. J. Singh and I. I. Mazin, 1997 *Phys. Rev. B*, **56**, R1650.
- [25] D. Parker and D. J. Singh, 2010, *Phys. Rev. B*, **82**, 035204.
- [26] G. K. H. Madsen, K. Schwarz, P. Blaha and D. J. Singh, 2003, *Phys. Rev. B*, **68**, 125212.
- [27] L. Zhang, M. -H. Du and D. J. Singh, 2010, *Phys. Rev. B*, **81**, 075117.
- [28] Mette S. Schmkel, et. al, 2014, *Chem. Sci.*, **5**, 1408.
- [29] M. Born, K. Huang, *Dynamical Theory of Crystal Lattices*, Clarendon, Oxford, 1954.
- [30] E. Guler and M. Guler, 2015 , *CHINESE JOURNAL OF PHYSICS*, **53**, 2.
- [31] Vijay Kumar Gudelli, V. Kanchana, S. Appalakondaiah, G. Vaitheeswaran and M. C. Valsakumar, 2013, *J. Phys. Chem. C* , **117**, 21120.
- [32] T NaKamura, 1981, *Japanese Journal of applied Physics*, **20**, 9.
- [33] Je-Hyeong Bahk and Ali Shakouri, 2016, *Phys. Rev. B*, **93**, 165209
- [34] Tribhuwan Pandey and Abhishek K. Singh, 2015, *Phys. Chem. Chem. Phys*, **17**, 16917
- [35] Hongliang Shi et. al, DOI: 10.1103/PhysRevApplied.3.014004
- [36] Sutarno, et. al, 1967, *Can. J. Chem.* **45** 1391-1400.
- [37] W. N. STASSEN and R. D. HEYDING, 1968, *Canadian Journal of Chemistry*, **46**, 2159
- [38] Sandip Dey and Vimal K. Jain, 2004 *Platinum Metals Rev.*, **48**, 16.

Table 1. Calculated bond length and bond angle in OsX_2 (X= S, Se, Te)

paramaters	OsS_2	OsSe_2	OsTe_2
$d(\text{Os-X})(\text{\AA})$	2.39	2.50	2.70
$d(\text{Os-Os})(\text{\AA})$	4.02	4.25	4.61
$(\text{Os-X-Os})(\text{deg})$	115.26	116.61	117.30

Table 2. Ground state properties of OsX_2 (X= S, Se, Te)

paramaters	OsS_2	OsSe_2	OsTe_2
$a_{pre}(\text{\AA})$	5.68	6.02	6.53
$a_{exp}(\text{\AA})$	5.6196[36]	5.946[37]	6.397[38]

Table 3. Calculated band gaps of OsX_2 (X=S,Se,Te) in eV

	OsS_2	OsSe_2	OsTe_2
	Present		
GGA	0.21	0	0
TB-mBJ	0.5	0.02	0
TB-mBJwith parameter	0.98	0.41	0.53

Table 4. Calculated effective masses of OsX_2 along different high symmetric directions in the unit of electron rest mass

Directions	OsS_2	OsSe_2	OsTe_2
VB (valence band)			
Γ -X	6.03	5.76	4.53
CB (conduction band)			
Γ -X	0.36	0.32	0.37

Table 5. Calculated elastic constants of OsX_2 (X=S,Se,Te)

parameters	OsS_2	OsSe_2	OsTe_2
$C_{11}(\text{GPa})$	449.653	481.477	426.226
$C_{12}(\text{GPa})$	55.650	57.936	36.464
$C_{44}(\text{GPa})$	107.321	143.651	151.963
B (GPa)	186.98	199.11	166.38
V_l (in Km/s)	6.33	6.31	6.05
V_t (in Km/s)	3.85	3.98	3.97
θ (in K)	511.54	496.14	454.652

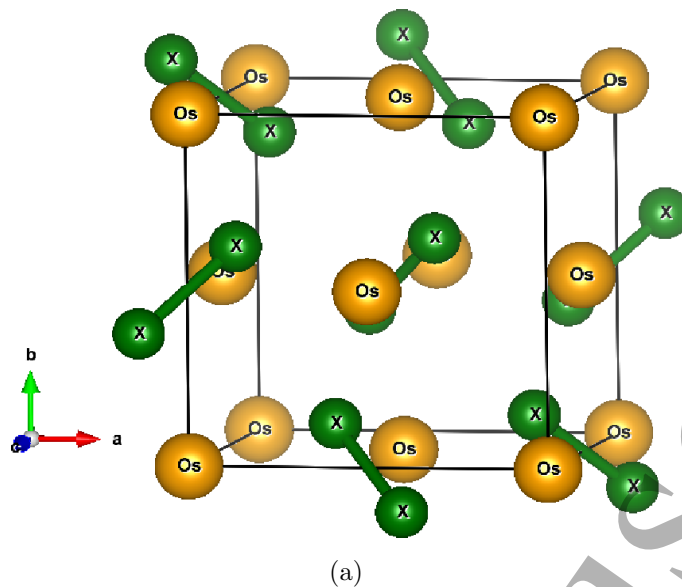


Figure 1. (Color online) Crystal structure of OsX_2 .

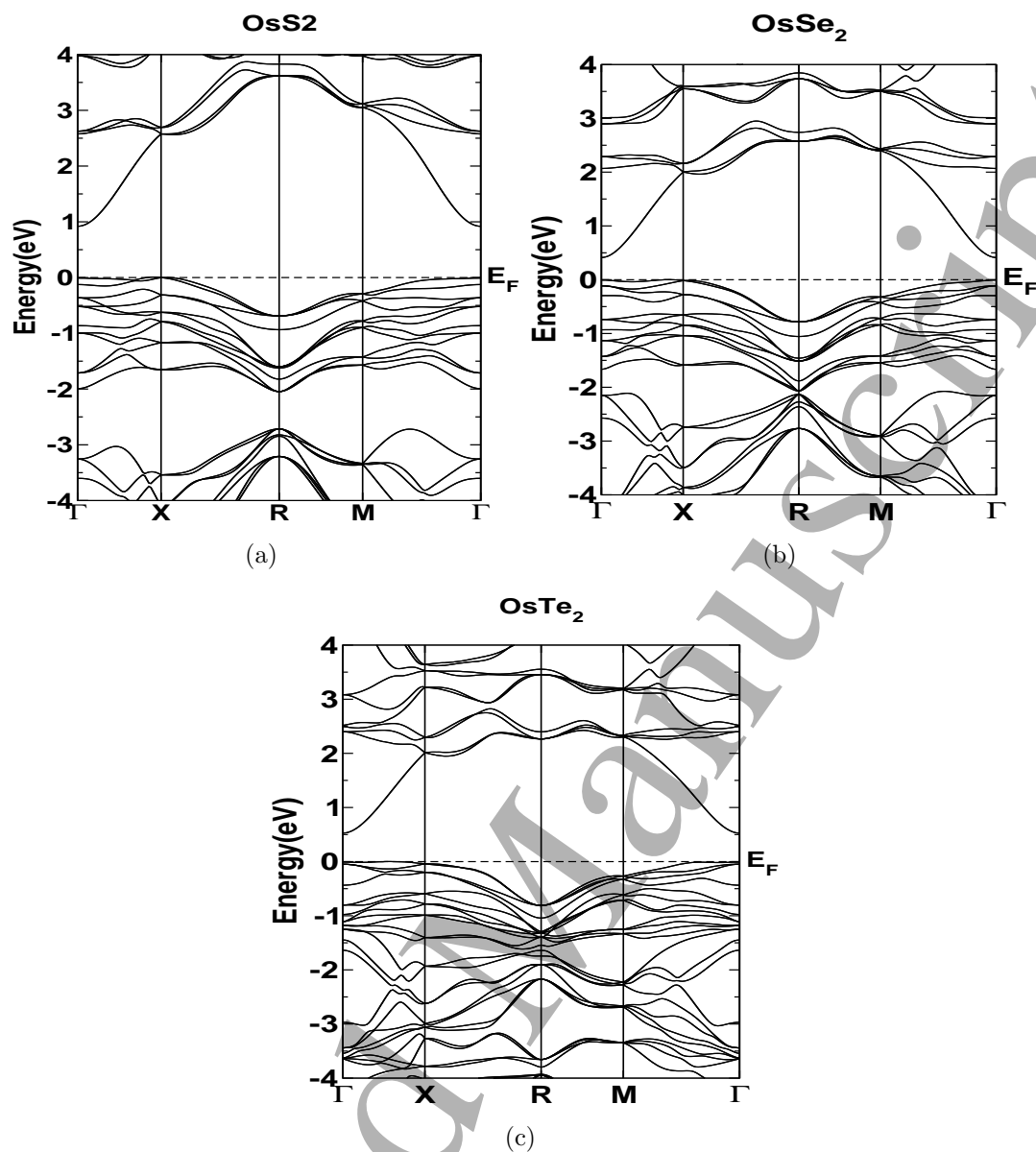


Figure 2. (Color online) Calculated band structure for (a) OsS₂ (b) OsSe₂ (c) OsTe₂

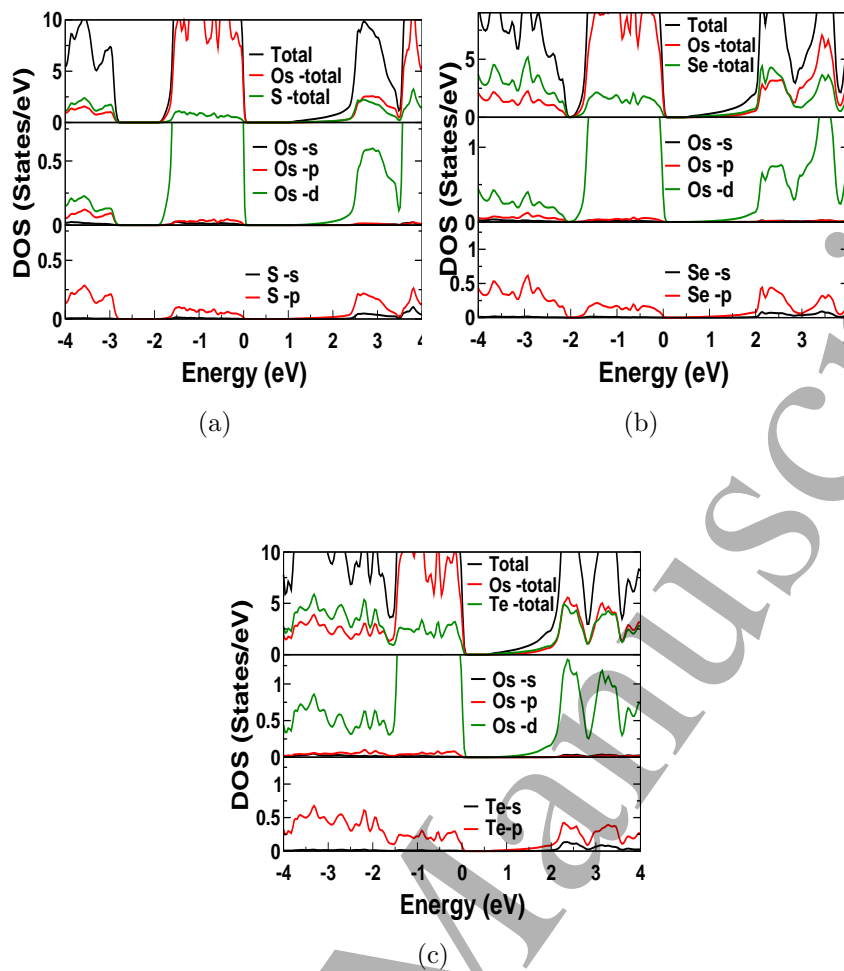


Figure 3. (Color online) Calculated density of states of all the compounds a)OsS₂, b)OsSe₂, c)OsTe₂

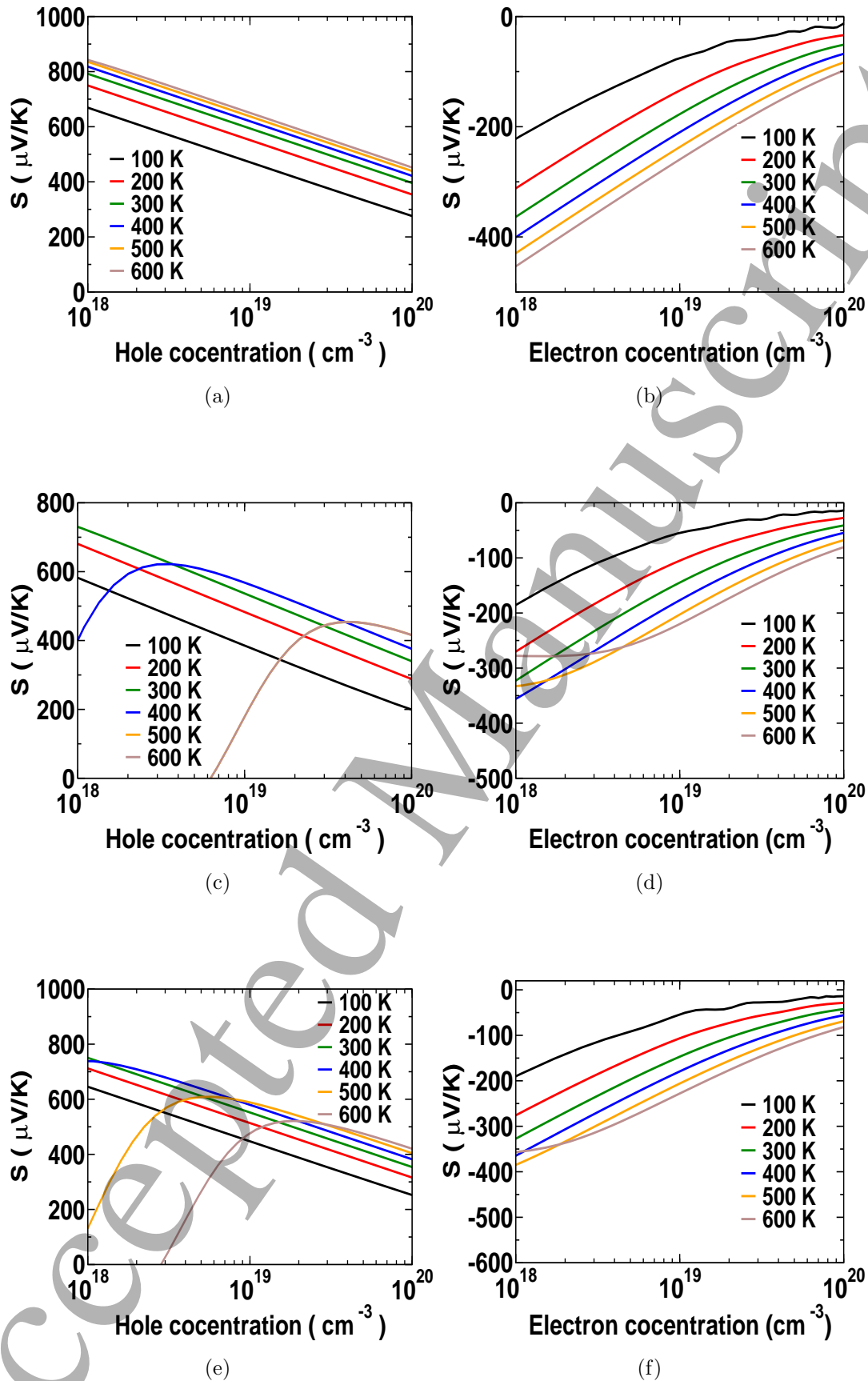


Figure 4. (Color online) Variation of thermopower as a function of carrier concentration for all the investigated compounds (a, b) OsS_2 (c,d) OsSe_2 , (e,f) OsTe_2

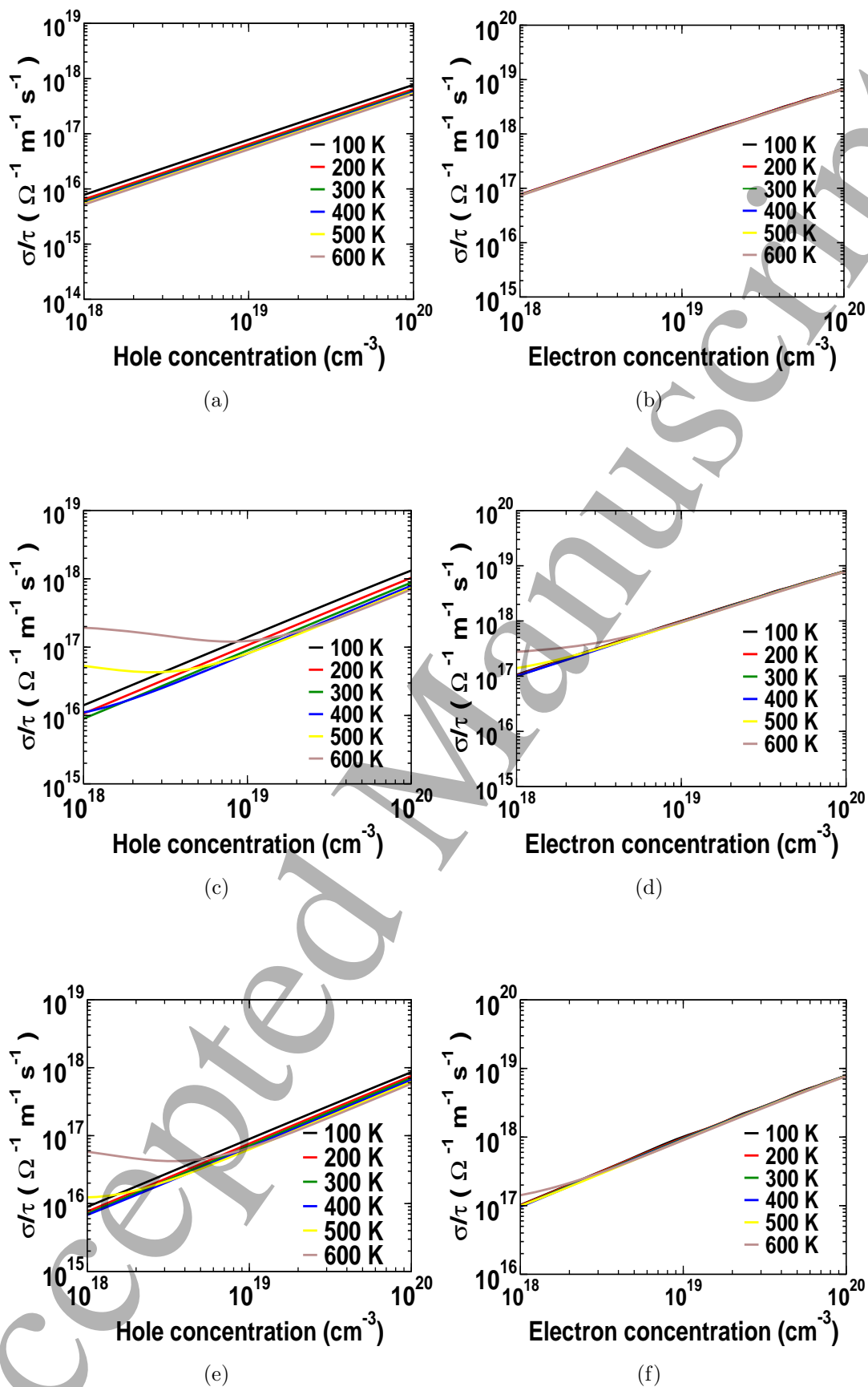


Figure 5. (Color online) Variation of electrical conductivity scaled by relaxation time as a function of carrier concentration of all the investigated compounds (a,b) OsS_2 , (c, d) OsSe_2 , (e,f) OsTe_2

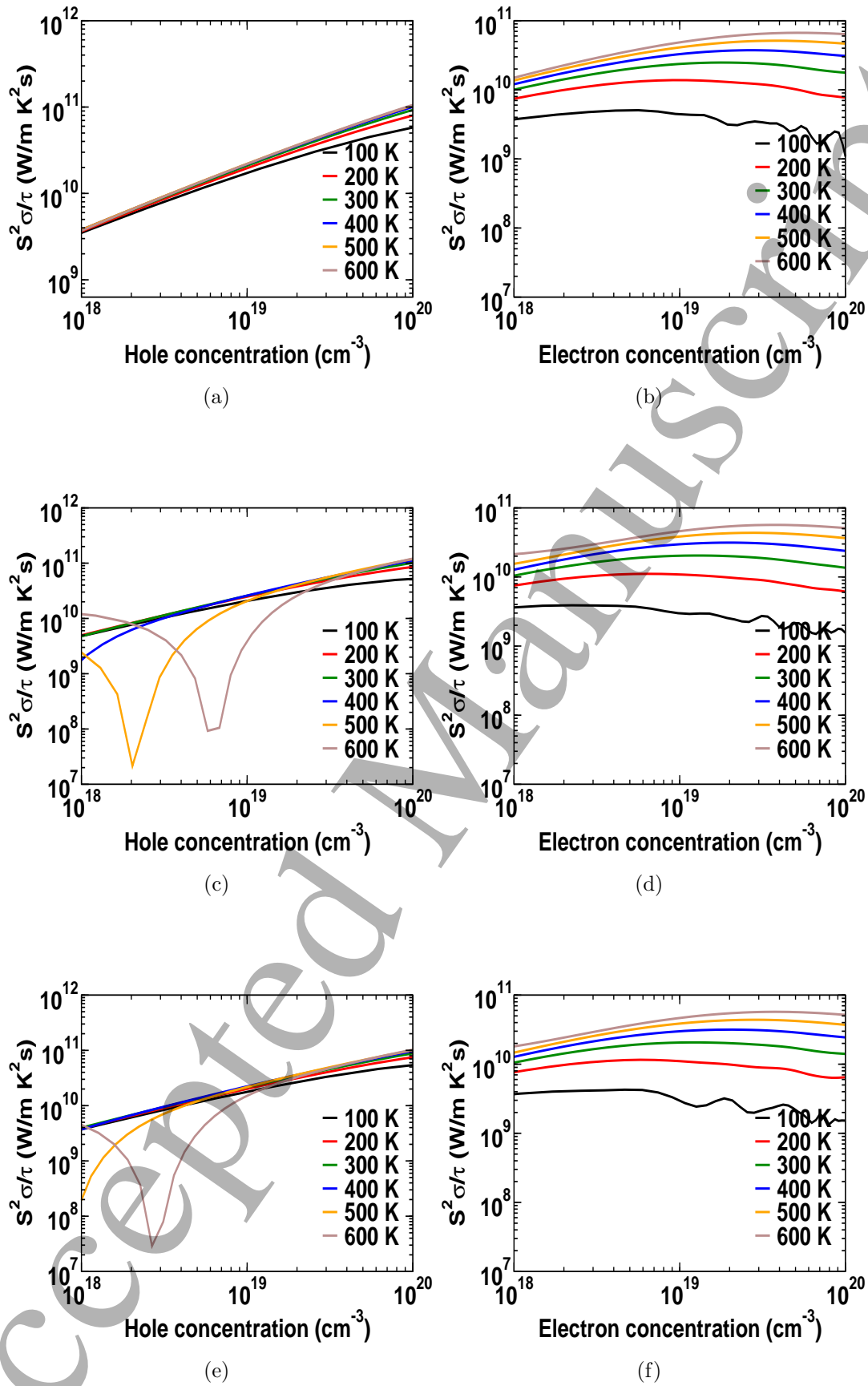


Figure 6. (Color online) Variation of power-factor as a function of carrier concentrations for all the compounds (a,b) OsS_2 , (c,d) OsSe_2 , (e, f) OsTe_2

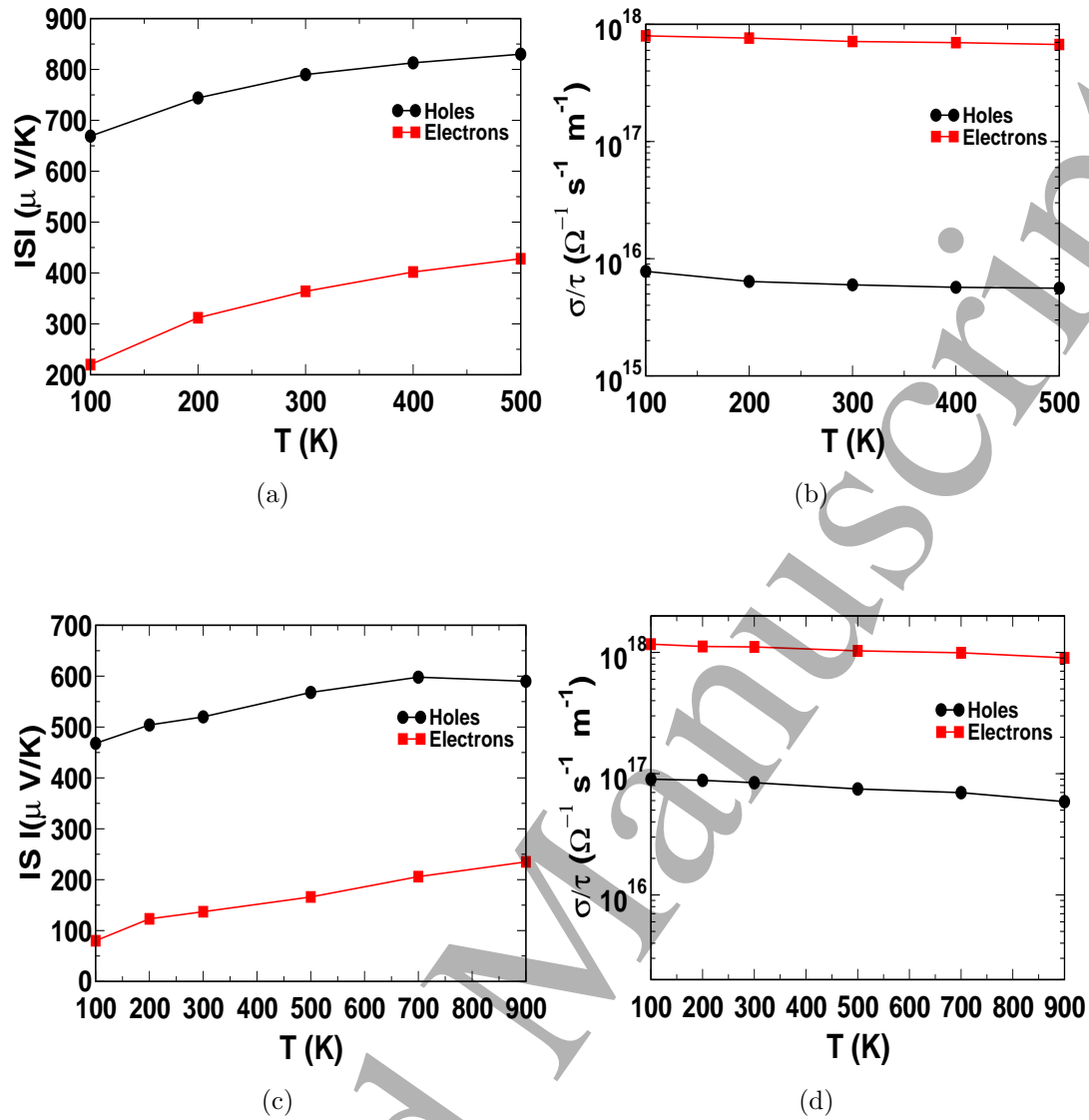


Figure 7. (Color online) Thermopower and electrical conductivity at different temperature for OsS₂ a)thermopower b) electrical conductivity at concentration around 10^{18}cm^{-3} , c)thermopower d) electrical conductivity at concentration around 10^{19}cm^{-3} concentrations

(a)

Figure 8. (Color online) Comparison with other compounds, OsX_2 (X: S, Se, Te), FeS_2 [31], Bi_2Te_3 [35], OsSb_2 , OsAs_2 [10]

Accepted Manuscript